Constraining the charge of a black hole with electromagnetic radiation from a black hole-neutron star system

Hao-Yu Yuan,[1,2] Hou-Jun Lü,[1,*] Jared Rice,[3] and En-Wei Liang[1]

[1]*Guangxi Key Laboratory for Relativistic Astrophysics, School of Physical Science and Technology, Guangxi University, Nanning 530004, China*
[2]*Department of Astronomy, School of Physics, Huazhong University of Science and Technology, Wuhan, 430074, China*
[3]*Department of Mathematics and Physical Science, Southwestern Adventist University, Keene, Texas 76059, USA*

Black hole-neutron star (BH-NS) mergers are expected to emit gravitational wave (GW) and electromagnetic (EM) counterparts when the NS is tidally disrupted or plunges into the BH. Recently, GW 200105 and GW200115 were claimed as originating in BH-NS mergers, even GW 200105 remains in debate. Several optical source candidates are reported to possible associate with the two GW events, but not confirmed yet. In this work, we assume that the BH is charged (the NS is naturally charged) and try to constrain the charge of the BH by using the possible associated EM emission from the charged BH and NS system working in the inspiral regime. We adopt electric and magnetic dipole radiations for the binaries which power a Poynting-flux-dominated outflow to accelerate electrons. Then, it produces the observed EM radiation via synchrotron radiation. We find that the conversion efficiency in the x-ray band is much higher than that of the ultraviolet, near-infrared, and radio bands. The estimated maximum charge-to-mass ratio (the charge for unit mass) of the BH is 1.12×10^{-6} and 1.53×10^{-6} esu for the binary systems of GW200105 and GW200115, respectively, if magnetic field strength $B_p \lesssim 10^{16}$ G and period $P > 1$ ms for the NS spin.

I. INTRODUCTION

Compact binary coalescences, including black hole-black hole (BH-BH), black hole-neutron star (BH-NS), and neutron star-neutron star (NS-NS) mergers, are expected to be a strong source for the production of gravitational wave (GW) radiation in the Universe (see [1] for a review). Catching the GW signal from such binary systems is the main target of current ground-based GW detectors, e.g., advanced Laser Interferometer Gravitational-Wave Observatory [LIGO; [2]], advanced Virgo Interferometer [Virgo; [3]], and KAGRA [4]. The first detected GW signals from the two events, GW 150914 and GW 151226 with LIGO, are proposed to be black hole binary mergers [5]. More interestingly, weak electromagnetic (EM) transients associated with the two GW events in the γ-ray band were claimed to be detected, but this is still highly debated [6–8]. On 17 August 2017, advanced LIGO and Virgo first directly detected both the GW signal (GW170817) and its EM counterparts (e.g., GRB 170817A and kilonova AT2017gfo) from the proposed merger of a binary NS system [9–16].

Despite the growing number of detected GW events, only several candidate BH-NS mergers have been reported,

namely GW190426 [17], GW190814 [18], GW190917 [19], GW191219 [20], and GW200210 [21]. Recently, GW 200105 and GW200115 were claimed as originating from the merger of BH-NS systems by the LIGO-Virgo-KAGRA (LVK) Collaboration during the third observing run (O3) stage [22], even GW200105 remains in debate. Unfortunately, no conclusive EM counterparts have been detected yet, except for several possible optical source candidates associated with the two GW events [23–30].

Whether or not EM counterparts accompany BH-NS mergers remains an open question. From the theoretical point of view, NSs can be tidal disrupted if the tidal disruption radius of the NS is larger than the innermost stable circular orbit radius of the BH and the massive debris can be expelled or accreted onto the newborn BH to power the EM counterparts [31,32]. However, the results of numerical simulations have shown that the conditions for NS disruption within inspiraling BH-NS binaries are extremely strict. For example the NS equations of state (EOS) need to be stiff enough or the BH spin projected to the orbital angular momentum needs to be extremely large [33,34]. On the other hand, the observed GW and EM data from LIGO, Virgo, and other telescopes are not likely to support the stiff NS EOS and the extremely high BH spin [35–39]. Given the observational evidences, NSs

plunging into the BHs during BH-NS mergers seems to be a natural physical processes during stellar evolution.

Within in this scenario, Ref. [40] proposed that EM radiation associated with the GW signal of the BH-NS merger can be produced if at least one of the members of BH-NS merger is charged. The system can raise intense electric-dipole and magnetic-dipole radiation near the orbital plane, and it propagates outward with a Poynting-flux-dominated outflow [40]. Finally, magnetic energy is dissipated to accelerate the electrons and can power the EM radiation with different radiation mechanisms (e.g., synchrotron radiation). On the other hand, the physical properties of a BH can be described simply with three parameters (mass, angular momentum, and charge). The mass and angular momentum of the BH can be roughly measured based on abundant observational data, but the charge of a BH is poorly understood [41–43]. Motivated by Ref. [40], one interesting question is whether or not we can constrain the charge of the BH using either the observed EM radiation or radiation upper limits in the BH-NS binary system if we assume that the BH is charged.

In this paper, we try to constrain the charge of BHs using the observed upper limits of EM radiation for GW200105 and GW200115 by assuming the BHs in the BH-NS systems are charged. We organize this paper as follows. The theoretical derivation of EM counterpart production during the merger of a NS with a charged BH is presented in Sec. II. In Sec. III, we describe the observations of GW200105 and GW200115. The constrained results are shown in Sec. IV. The conclusions are drawn in Sec. V with some additional discussions. Throughout this paper, we use cgs units and adopt a concordance cosmology with parameters $H_0 = 67.4 \ \mathrm{km \, s^{-1} \, Mpc^{-1}}$, $\Omega_M = 0.315$, and $\Omega_\Lambda = 0.685$ [44].

II. GENERAL THEORY OF CHARGED BH-NS MERGERS

A. Electric-dipole and magnetic-dipole radiations

Two different channels for the formation of a BH-NS system are discussed in literatures [45–47], but they are remaining in debate. One is binary systems with each member of the binary undergoing massive star collapse when the thermal force of the star can not support its gravitational force [for a review [45,46]]. The other one is the dynamical interactions between BHs and NSs in globular clusters which contain many compact stars (e.g., BH and NS). Then, these interactions can produce the binary systems that contain two or more compact objects [47].

After the BH-NS binary is formed, the orbital separation between the objects gradually decreases until coalescence because of the energy loss due to GW emission. The NS has a strong surface magnetic field and a rapid rotation, and its surface magnetic field changes with time as it is orbiting

with the BH. The changing NS magnetic field can produce an electric field, so that both a magnetic field and an electric field live on the surface of the NS. For our BH-NS system, we assume that NS plunges into the BH without tidal disruption and that the BH is charged. If this is the case, the EM signals may be produced via both electric dipole and magnetic dipole radiation and propagate outward with a Poynting-flux-dominated outflow.

Following the method of Refs. [40,48], $M_i, \hat{q}_i$ are defined as the mass and relative charge of the BH or NS, respectively. Here, the subscript i represents either the BH or the NS. $\hat{q}_i$ is defined as the ratio Q_i/M_i [48], where Q_i and M_i are the absolute charge and mass of the BH or NS, and G is the gravitational constant. Moreover, we also define other parameters as follows:

$$\text{Total mass:} \ M = M_{\mathrm{BH}} + M_{\mathrm{NS}};$$
$$\text{Mass ratio:} \ q = M_{\mathrm{BH}}/M_{\mathrm{NS}};$$
$$\text{Reduced mass:} \ M_r = M_{\mathrm{BH}} M_{\mathrm{NS}}/(M_{\mathrm{BH}} + M_{\mathrm{NS}});$$
$$\text{Chirp mass:} \ M_c = M_r^{3/5} M^{2/5};$$
$$\text{Horizon mass:} \ M_h = M_r^{2/5} M^{3/5}.$$

The charged BH-NS system can give rise to electric dipole and magnetic dipole radiation due to the interaction between the magnetosphere of the binaries during inspiral. We present more details of both electric dipole and magnetic dipole radiation in the following.

(1) Luminosity of electric dipole radiation: In general, considering that just one member of a BH-NS binary is charged (e.g., NS is charged), the electric dipole radiation luminosity can be written as the Larmor formula [40,48,49],

$$\begin{aligned} L_{e,\mathrm{NS}} &= \frac{2 Q_{\mathrm{NS}}^2 |\ddot{r}_{\mathrm{NS}}|^2}{3 c^3} \\ &= \frac{1}{24} \frac{c^5}{G^2} \hat{q}_{\mathrm{NS}}^2 \left[\frac{r_s(M_{\mathrm{BH}})}{a} \right]^2 \left[\frac{r_s(M_{\mathrm{NS}})}{a} \right]^2, \quad (1) \end{aligned}$$

where c is speed of light, and $r_s(M_i) = \frac{2GM_i}{c^2}$. Hence, $r_s(M_{\mathrm{BH}})$ and $r_s(M_{\mathrm{NS}})$ are the Schwarzschild radii of the masses M_{BH} and M_{NS}, respectively. $|\ddot{r}_{\mathrm{NS}}| = \frac{GM_{\mathrm{BH}}}{a^2}$ is the amplitude of the acceleration of the NS and a is the separation of the BH-NS binary. Similarly, one may easily write the luminosity if only the BH is charged. However, if both NS and BH are charged, one should consider not only the contributions from charged NS and charged BH itself, but also the cross-term effect between the charged BH and charged NS. The total dipole moment of the system is $d = Q_{\mathrm{NS}} r_{\mathrm{NS}} + Q_{\mathrm{BH}} r_{\mathrm{BH}}$ by choosing the origin of coordinates at the center of mass, where r_{NS} and r_{BH} are the radius vector of

neutron star and black hole, respectively. Based to Larmor formula, one has

$$L_e = \frac{4}{3c^3}\ddot{d}^2 \qquad (2)$$

$$M_i \ddot{r}_i = \pm \frac{GM_{NS}M_{BH}}{r^2} \mp \frac{Q_{NS}Q_{BH}}{r^2}, \qquad (3)$$

where $r = r_{NS} - r_{BH}$ is the relative position of them. We can derive the luminosity of electric dipole radiation for both charged BH and charged NS by adopting $a \approx |r|$ [50–52],

$$L_e \approx \frac{4}{3}\frac{c^5}{G^2}(\hat{q}_{NS} - \hat{q}_{BH})^2 \left(1 - \frac{\hat{q}_{NS}\hat{q}_{BH}}{G}\right)^2$$
$$\times \left[\frac{r_s(M_{BH})}{2a}\right]^2 \left[\frac{r_s(M_{NS})}{2a}\right]^2. \qquad (4)$$

Here, we ignore the effect of EM force on the orbital evolution, and only consider the gravitational force between the BH and NS to calculate the orbital evolution of the systems, because the charge of BH is small enough. We compare with the luminosity between EM and GW at different radius for different charge, and derive the critical condition for the validity of this assumption. The GW luminosity is expressed as

$$L_{GW} = \frac{32}{5}\frac{G^4}{c^5}\frac{M_r^2 M^3}{a^5}f(e), \qquad (5)$$

where $f(e) = (1 + \frac{73}{24}e^2 + \frac{37}{96}e^4)/(1 - e^2)^{7/2}$ is a coefficient for elliptic orbits, and e is the orbital eccentricity. We adopt a reasonable value of $e = 0$ in the calculations below [40].[1]

In addition, the orbital separation a gradually decreases due to the energy loss of GW emission during inspiral, and the rate of change of a can be written as

$$\frac{da}{dt} = -\frac{64}{5}\frac{G^3}{c^5}\frac{M_{NS} \cdot M_{BH}(M_{NS} + M_{BH})}{a^3}f(e)$$
$$= -\frac{64}{5}\frac{G^3}{c^5}\frac{M_r M^2}{a^3}f(e). \qquad (6)$$

---

[1]The orbital eccentricity is decreasing during inspiral, and it would be close to zero due to GW or EM radiations, and ejected energy (the electric dipole and magnetic dipole radiations) are close to maximum values with the increasing of orbital frequency when the orbital eccentricity is close to zero. Thus, the ejected energy at this stage can represent the total energy which ejected during the inspiral and coalescence. Combining these accounts, orbital eccentricity equal to zero is a reasonable approximation [40].

(2) Luminosity of magnetic dipole radiation: When a charged BH-NS binary inspiral, a loop current can be produced because of the interaction between their magnetospheres. Generally speaking, BH is considered to be electrically neutral. However, if the BH is in the nonelectricity neutral environment or formed in the strong magnetic fields, the BH would be charged and generated magnetospheres [50,53]. In classical electromagnetism, the magnetic dipole moment is the product of the current and effective area of the loop [48],

$$\mu = \frac{\pi}{c}I\left(\frac{a}{2}\right)^2 = \sqrt{GMa}\frac{Q_{BH} + Q_{NS}}{8c}, \qquad (7)$$

where $I = (Q_{BH} + Q_{NS})/P_s$ is the loop current, and $P_s = 2\pi a^{3/2}/\sqrt{GM}$ is the orbital period [54,55]. The luminosity of magnetic dipole radiation can be expressed as

$$L_m = \frac{2\ddot{\mu}^2}{3c^3}$$
$$\approx 8.56 \times 10^2 \frac{G^{13}M_r^4 M^9}{c^{25}a^{15}}(\hat{q}_{BH} \cdot M_{BH} + \hat{q}_{NS} \cdot M_{NS})^2, \qquad (8)$$

where $\ddot{\mu}$ is the second derivative of magnetic dipole moment.

B. Calculation of the charge of a NS

Reference [56] proposed the distribution of spatial charge density (ρ_e) of a magnetized NS, $\rho_e = -\mathbf{\Omega} \cdot \mathbf{B}/(2\pi c)$, where $\mathbf{\Omega}$ and $\mathbf{B}$ are the angular velocity and magnetic field strength of the NS, respectively. Assuming that the surface magnetic field of the NS is a dipole field, $B = B_p R_{NS}^3/(r^3)(3\cos^2\theta + 1)^{1/2}$, we adopt a simple situation that $\mathbf{\Omega} \cdot \mathbf{B} < 0$. The charge of the NS ($Q_{NS}$) consists of two parts; the charge within the magnetosphere (Q_{mag}) and inside the NS (Q_{in}). For Q_{mag}, one needs to integrate along the distance from the NS surface (R_{NS}) to r, which is the distance between the reference point and the NS center,

$$Q_{mag} = \int_0^{2\pi}\int_0^\pi\int_{R_{NS}}^r -\frac{\mathbf{\Omega} \cdot \mathbf{B}}{2\pi c}r^2 \sin\theta \, dr d\varphi d\theta$$
$$= \frac{\Omega B_p R_{NS}^3}{c}\int_{R_{NS}}^r \frac{1}{r}dr \int_0^\pi \cos\theta \sin\theta \sqrt{3\cos^2\theta + 1}\,d\theta, \qquad (9)$$

where B_p is the strength of surface dipole magnetic field of the NS, and θ is azimuthal angle. Because the antisymmetry of the integrand around $\pi/2$ for the integral over θ, one can guarantee that the value of integrating for θ is zero, namely, $Q_{mag} = 0$. Similarly, if the NS is uniformly magnetized, one can calculate Q_{in} as [57],

$$Q_{\mathrm{in}} = \frac{2}{3}\Omega B_p R_{\mathrm{NS}}^3. \tag{10}$$

The total charge of the NS depends on the properties of the NS (e.g., angular velocity, dipole magnetic-field strength, and the radius), and can be written as

$$Q_{\mathrm{NS}} = Q_{\mathrm{mag}} + Q_{\mathrm{in}}. \tag{11}$$

C. Synchrotron radiation of Poynting-flux-dominated outflow

In this section, we will discuss how the BH-NS system will radiate energy. For either magnetic dipole or electric dipole radiation, the radiation frequency is equal to the orbital frequency of ~kHz. However, the orbital frequency is much lower than the intrinsic frequency of interstellar medium (~10^4 Hz [58]). Here, we do not consider the affect of the high interstellar medium (~1 cm^{-3}). The intrinsic (or oscillation) frequency of interstellar medium (~$10^4 n_e^{1/2}$ Hz) originates from the thermal motion of electrons within the Debye length, where n_e is the electron number density per cm^3 in the interstellar medium. The low-frequency electromagnetic radiation can be prevented from propagating when EM frequency is less than the intrinsic frequency of interstellar medium. Therefore, it is inevitable that the radiation would be trapped in the vicinity of the binary. In practice, the energy of the dipole radiation can propagate outward with a Poynting-flux-dominated outflow. The Poynting luminosity at a radius (r_p) is written as [59,60]

$$\begin{aligned} L_p &= c\frac{(r_p B_{\mathrm{jet}})^2}{4\pi} \\ &= (L_e + L_m)\left(1 - \frac{\Gamma}{\Gamma_{\mathrm{sat}}}\right) \\ &= L_{\mathrm{tot}}\left(1 - \frac{\Gamma}{\Gamma_{\mathrm{sat}}}\right), \end{aligned} \tag{12}$$

where B_{jet} and Γ are the jet magnetic field strength and bulk Lorentz factor within the outflow, respectively.

The total energy from the electric-dipole and magnetic-dipole radiation ($L_{\mathrm{tot}} = L_e + L_m$) is used to inject the outflow, and Γ_{sat} is the bulk Lorentz factor at the saturation radius r_{sat} of the outflow. Subsequently, the magnetic energy will be dissipated gradually via magnetic reconnection to accelerate electrons. Moreover, particle-in-cell simulations suggest that the energy spectrum of accelerated electrons is roughly a power-law distribution [61–63],

$$N(\gamma_e)d\gamma_e \propto \gamma_e^{-p}d\gamma_e, \qquad \gamma_e \geq \gamma_m, \tag{13}$$

where γ_e and γ_m are the Lorentz factor and minimum Lorentz factor of accelerated electrons, respectively, and p is the power-law index of accelerated electrons. Here, we

adopt $p = 4\sigma^{-0.3}$ according to a reasonable fit for the results of numerical calculations, and σ is the magnetization parameter of the outflow. Qualitatively, it is the ratio between magnetic energy and kinetic energy in the outflow, namely $\sigma = L_p/L_k$. As the energy of accelerated electrons is dissipated, it can produce broadband radiation via different radiation mechanisms (e.g., synchrotron radiation and inverse Compton scattering). In this paper, we consider only the pure synchrotron radiation[2] which can generate multiband afterglow of GRBs (from x-ray to radio, [59,65]).

Reference [66] considered a relativistic shock propagating through a uniform cold medium, and assumed that the shock undergoes adiabatic and radiative hydrodynamic evolution. Within this scenario, they calculated the radiated spectrum for two different regions, e.g., fast-cooling and slow-cooling cases. In order to distinguish those two spectral regions, one defines a parameter γ_c which is the critical Lorentz factor for electron-synchrotron radiation. The energy loss through synchrotron radiation becomes significance when the minimum Lorentz factor of electrons exceed the threshold exceed. So that, one can separates those two regions by comparing with γ_c, e.g., $\gamma_m > \gamma_c$ (fast cooling) and $\gamma_m < \gamma_c$ (slow cooling). We list the luminosity (L_ν) at each frequency (ν) as follows for these two cases.

(1) Fast-cooling regime:

$$L_\nu = \begin{cases} L_{\nu,\mathrm{max}}\left(\frac{\nu}{\nu_c}\right)^{\frac{1}{3}}, & \nu < \nu_c \\ L_{\nu,\mathrm{max}}\left(\frac{\nu}{\nu_c}\right)^{-\frac{1}{2}}, & \nu_c < \nu < \nu_m \\ L_{\nu,\mathrm{max}}\left(\frac{\nu_m}{\nu_c}\right)^{-\frac{1}{2}}\left(\frac{\nu}{\nu_m}\right)^{-\frac{p}{2}}, & \nu_m < \nu < \nu_{\mathrm{max}} \end{cases} \tag{14}$$

(2) Slow-cooling regime:

$$L_\nu = \begin{cases} L_{\nu,\mathrm{max}}\left(\frac{\nu}{\nu_m}\right)^{\frac{1}{3}}, & \nu < \nu_m \\ L_{\nu,\mathrm{max}}\left(\frac{\nu}{\nu_m}\right)^{-\frac{p-1}{2}}, & \nu_m < \nu < \nu_c \\ L_{\nu,\mathrm{max}}\left(\frac{\nu_c}{\nu_m}\right)^{-\frac{p-1}{2}}\left(\frac{\nu}{\nu_c}\right)^{-\frac{p}{2}}, & \nu_c < \nu < \nu_{\mathrm{max}} \end{cases} \tag{15}$$

where $L_{\nu,\mathrm{max}}$, ν_m, ν_c, and ν_{max} correspond to the maximal luminosity, typical frequency, cooling frequency, and the maximal frequency, respectively. The maximal synchrotron spectral luminosity,

$$\begin{aligned} L_{\nu,\mathrm{max}} &= \frac{m_e c^2 \sigma_T B_{\mathrm{jet}} N_e}{3e} \\ &= \frac{m_e c^2 \sigma_T N_e}{3e}\left[\frac{4\pi L_{\mathrm{tot}}}{c r_p^2}\left(1 - \frac{\Gamma}{\Gamma_{\mathrm{sat}}}\right)\right]^{1/2}, \end{aligned} \tag{16}$$

---

[2]The synchrotron radiation is the main radiation mechanism in GRB study via the observational data [64]. Here, we do not consider other radiation mechanisms, such as curvature radiation, Compton scattering, and inverse Compton scattering.

TABLE I.   Properties of BH-NS merger events and their candidate objects.

GW event	$M_{NS}(M_\odot)$	$M_{BH}(M_\odot)$	Redshift	Mass ratio (q)	Chirp mass($M_\odot$)
GW200105	$1.9^{+0.2}_{-0.2}$	$8.9^{+1.1}_{-1.3}$	$0.06^{+0.02}_{-0.02}$	$0.21^{+0.03}_{-0.04}$	$3.41^{+0.08}_{-0.07}$
GW200115	$1.4^{+0.6}_{-0.2}$	$5.9^{+1.4}_{-2.1}$	$0.07^{+0.03}_{-0.02}$	$0.24^{+0.12}_{-0.09}$	$2.42^{+0.05}_{-0.07}$
GW190426	$1.5^{+0.8}_{-0.5}$	$5.7^{+3.9}_{-2.3}$	$0.08^{+0.04}_{-0.03}$	$0.26^{+0.23}_{-0.14}$	$2.41^{0.08}_{-0.08}$
GW190814	$2.59^{+0.08}_{-0.09}$	$23.2^{+1.1}_{-1.0}$	$0.050^{+0.009}_{-0.010}$	$0.11^{+0.01}_{-0.01}$	$6.09^{+0.06}_{-0.06}$
GW190917	$2.1^{+1.5}_{-0.5}$	$9.3^{+3.4}_{-4.4}$	$0.15^{+0.06}_{-0.06}$	$0.23^{+0.18}_{-0.12}$	$3.7^{+0.2}_{-0.2}$
GW191219	$1.17^{+0.06}_{-0.05}$	$31.6^{+1.8}_{-2.5}$	$0.11^{+0.04}_{-0.03}$	$0.037^{+0.003}_{-0.003}$	$4.33^{+0.10}_{-0.15}$
GW200210	$2.79^{+0.54}_{-0.48}$	$24.5^{+8.9}_{-5.3}$	$0.19^{+0.07}_{-0.06}$	$0.11^{+0.05}_{-0.03}$	$6.56^{+0.34}_{-0.38}$

where σ_T, e, and N_e are the Thomson scattering cross section, the electron charge, and the total number of emitting electrons in the jet at r_p, respectively. Equations (14) and (15) are invalid as long as the frequency is below the synchrotron self-absorption (SSA) frequency ν_a, and

$$\frac{2\nu_a^2}{c^2}\gamma_a \Gamma m_e c^2 \frac{\pi r_p^2}{\Gamma^2} = L_{\nu_a}, \qquad (17)$$

where m_e and γ_a are the electron mass and Lorentz factor corresponding to ν_a, respectively. The SSA effect might play an important role when $\nu < \nu_a$, and the spectral shape become $L_\nu \propto \nu^{11/8}$ [67].

III. OBSERVATIONS OF THE GW200105 AND GW200115 EVENTS

During the third observing run (O3), the LVK reported that two GW events (GW200115 and GW200105) are originated from BH-NS binaries [22], but the GW 200105 remains in debate later due to the high likelihood of detector noise [68]. Based on the GW signals from the two events, the inferred mass of their primary are $8.9^{+1.2}_{-1.5}M_\odot$ and $5.7^{+1.8}_{-2.1}M_\odot$, respectively. These primary masses are well in excess of the maximum NS mass, but fall into the mass range of BHs. On the other hand, the mass of the companions are $1.9^{+0.3}_{-0.2}M_\odot$ and $1.5^{+0.7}_{-0.3}M_\odot$, respectively. These are consistent with the mass range of known NSs and are below the maximum NS mass. Moreover, the LVK Collaboration claims that GW observations of LIGO and Virgo have led to the identification of five BH-NS candidates, GW190426 [17], GW190814 [18], GW190917 [19], GW191219 [20], and GW200210 [21]. The inferred primary mass, secondary mass, chirp mass, mass ratio, and redshift are collected in Table I for these GW events and their candidate BH-NS merger objects.

Searching for the EM counterparts of a BH-NS merger has so far remained main targets and expectations of space and ground telescopes. There are no EM counterparts associated with the GW candidates of BH-NS merger that were claimed by the LVK Collaboration. For the GW200105 and GW200115 events, no significant signals

were caught in the $\gamma-$ray band above the background because of the short-duration and rapid decline of the expected short GRB.[3] [69–87]. However, the Swift/XRT team claimed that several possible x-ray emission candidates within the localization area of the GW trigger S200115j were caught [88,89]. Afterwards, possible associated optical/IR observations have been reported within an error box larger than that of the error boxes of GW200105 and GW200115, though they cannot be confirmed.

Global MASTER-Net telescopes started to scan the GW200105 error box ∼3.2 hours after the GW trigger, and got a series of upper limits in V- and C-band [90].[4] The Zwicky Transient Facility (ZTF) inspected the localization area that covered ∼51.7% of the enclosed area of the GW trigger S200105ae in the g- and r-band, and reported more than 20 optical transients as the possible EM candidates of GW200105 [91,92], although several other observations stated that there are five candidates that actually are consistent with supernovae (SNe) [93–95]. For GW200115, the ZTF and Global Relay of Observatories Watching Transients Happen (GROWTH) Collaborations accidentally observed the localization region of the GW trigger S200115j and covered 22% of the localization probability [96]. Srivastav and Smartt [97] also reported the transients within one of the eastern lobes of this trigger with the Pan-STARRS2 telescope. The optical/IR observations reported by GCN are summarized in Tables II and III.

IV. RESULTS

To date, there is indeed not directly evidence to observe the EM counterparts of BH-NS systems, only report the optical candidates or upper limits of EM counterparts in the two events GW200105 and GW200115. If this is the case, one can constrain the BH charge according the hypothesis of charged BH-NS systems by adopting the upper limits. In this section, we assume that either the observed optical transients above or even upper limits as the EM

---

[3]The other possibility is that no gamma-ray signals were produced when they are in nondisrupting systems.
[4]C-band is a clear (unfiltered) band.

TABLE II. EM candidates for GW200105.

Detector	Object name	RA	Declination	Filter	Magnitude (AB)
ZTF[a]	ZTF20aaervoa/AT2020pp	15 h 02 m 38.38 s	+16 d 28 m 21.5 s	r	20.08
	ZTF20aaertpj/AT2020pv	14 h 27 m 52.03 s	+33 d 34 m 09.7 s	r	19.55
	ZTF20aaervyn/AT2020pq	15 h 01 m 27.45 s	+20 d 37 m 23.5 s	r	20.49
	ZTF20aaerqbx/AT2020ps	15 h 49 m 26.29 s	+40 d 49 m 55.0 s	r	19.70
	ZTF20aaerxsd/AT2020py	14 h 00 m 54.27 s	+45 d 28 m 21.8 s	r	19.97
	ZTF20aaexpwt/AT2020adi	06 h 26 m 01.30 s	+11 d 33 m 38.85 s	r	19.80
	ZTF20aaertil/AT2020pu	14 h 52 m 25.86 s	+31 d 01 m 18.50 s	g	19.70
	ZTF20aaevbzl/AT2020adf	13 h 26 m 41.27 s	+30 d 52 m 30.68 s	g	20.30
	ZTF20aagiipi/AT2020adl	15 h 33 m 24.61 s	+42 d 02 m 36.70 s	r	20.10
	ZTF20aagijez/AT2020adm	15 h 04 m 13.18 s	+27 d 29 m 04.19 s	r	19.90
	ZTF20aagiiik/AT2020abl	16 h 19 m 09.94 s	+53 d 45 m 38.26 s	r	20.30
	ZTF20aafexle/AT2020adn	04 h 20 m 31.22 s	−09 d 30 m 28.20 s	r	19.90
	ZTF20aaflndh/AT2020xz	01 h 22 m 38.14 s	−06 d 49 m 34.31 s	g	19.20
	ZTF20aafduvt/AT2020ado	03 h 36 m 28.54 s	−07 d 49 m 34.52 s	g	20.10
	ZTF20aafefxe/AT2020adt	07 h 47 m 24.18 s	+14 d 42 m 23.82 s	r	20.90
	ZTF20aafkkoy/AT2020adp	13 h 40 m 59.99 s	+40 d 48 m 49.03 s	r	19.30
	ZTF20aafaoki/AT2020adq	05 h 13 m 13.80 s	+05 d 09 m 56.55 s	r	19.60
	ZTF20aafujqk/AT2020adg	17 h 57 m 00.41 s	+10 d 32 m 20.31 s	r	18.60
	ZTF20aafksha/AT2020adr	13 h 43 m 54.45 s	+38 d 25 m 13.82 s	g	20.00
	ZTF20aagjemb/AT2020adh	14 h 51 m 25.85 s	+45 d 20 m 41.18 s	r	20.30
	ZTF20aafdxkf/AT2020ads	03 h 42 m 07.08 s	−03 d 11 m 39.05 s	r	20.20
	ZTF20aafukgx/AT2020adj	18 h 23 m 21.44 s	+17 d 49 m 31.65 s	r	19.20
	ZTF20aafanxk/AT2020adk	05 h 35 m 36.04 s	+11 d 46 m 15.31 s	r	19.40
GTC[b]	AT2020oo/Gaia20add	17 h 19 m 6.18 s	+25 d 27 m 20.23 s	r'	17.56
MASTER-SAAO[c]	/	04 h 16 m 26.77 s	−54 d 52 m 08.5 s	V	>16.00

[a]The observational data for this detector are collected from Stein *et al.* [91] and Ahumada [92].
[b]The observational data for this detector are collected from Hu *et al.* [98].
[c]This upper limit of the detector is collected from Lipunov *et al.* [90].

TABLE III. EM candidates for GW200115.

Detector	Object name	RA	Declination	Filter	Magnitude (AB)
ZTF[a]	ZTF20aafqpum/AT2020yo	03 h 06 m 06.50 s	+13 d 54 m 48.4 s	g	20.80
	ZTF20aafqulk/AT2020yp	03 h 39 m 45.43 s	+27 d 44 m 05.4 s	g	21.10
	ZTF20aafqvyc/AT2020yq	03 h 47 m 58.21 s	+38 d 26 m 31.8 s	g	20.90
Swift/UVOT[b]	S200115j_X136	02 h 40 m 12.19 s	−02 d 33 m 45.4 s	u	16.54
Pan-STARRS2[c]	PS20ev/AT2020ait	02 h 36 m 56.51 s	−02 d 12 m 03.5 s	w[*]	20.23
	PS20 fs/AT2020ajy	02 h 53 m 21.00 s	+03 d 23 m 17.4 s	w	21.46
	PS20fo/AT2020ajw	02 h 25 m 53.75 s	−03 d 13 m 04.6 s	w	19.90
	PS20fr/AT2020ajx	02 h 25 m 23.51 s	−07 d 50 m 15.5 s	w	20.42
	PS20fu/AT2020ajz	02 h 49 m 02.17 s	+04 d 59 m 11.6 s	w	21.16
	PS20fv/AT2020aka	02 h 37 m 24.50 s	−01 d 09 m 20.1 s	w	19.91
	PS20fw/AT2020akb	03 h 10 m 05.41 s	+05 d 59 m 16.4 s	w	21.05
	PS20f/AT2020akc	02 h 52 m 35.05 s	+07 d 15 m 11.9 s	w	20.89

[a]The "pivot" wavelength of the w-band is 0.608 μm [99].
[b]The relevant data are in Anand *et al.* [96].
[c]Swift/UVOT observational data are from Oates & Swift Team [100].
[d]The relevant data are in Srivastav & Smartt [97].

counterparts of GW200105 and GW200115 events, and adopt those observed EM counterparts to constrain the BH charge by given the hypothesis of a charged BH-NS system.

A. Conversion efficiency of electric-dipole and magnetic-dipole radiation

The charged BH and NS system can produce both electric dipole and magnetic dipole radiation due to the interaction between the magnetospheres of the objects during inspiral. The total energy from the electric dipole and magnetic dipole radiation (L_{tot}) is used to inject into the outflow, and it propagates outward with a Poynting-flux-dominated outflow. Within the synchrotron radiation scenario, the conversion efficiency (η) is defined as the ratio between the luminosity of the observed energy bands and total luminosity (e.g., the sum of electric and magnetic dipole radiation),

$$\eta = \frac{\int_{\nu_1}^{\nu_2} L_\nu d\nu}{L_{\text{tot}}}, \qquad (18)$$

where ν_1 and ν_2 are the frequency range of a certain energy band or detector, respectively.

The conversion efficiency is dependent on the frequency and the synchrotron radiation luminosity L_ν. For a given energy band, Eq. (18) can be calculated by adopting Eqs. (14), (15), and (17). Here, we adopt the $\Gamma_{\text{sat}} = \sigma_0 \Gamma_0 = \sigma_0^{3/2} = 1000$ to calculate the $L_{\nu,\text{max}}$, where Γ_0 and σ_0 are the initial Lorentz factor and magnetization parameter of the outflow, respectively. One can calculate the conversion efficiency as a function of the given total luminosity [65]. Figure 1 shows the conversion efficiency as function of L_{tot} from the x-ray to radio bands. It is clear to see that the conversion efficiency in the x-ray band is much higher than that of the ultraviolet (UV), near-infrared, and radio bands,
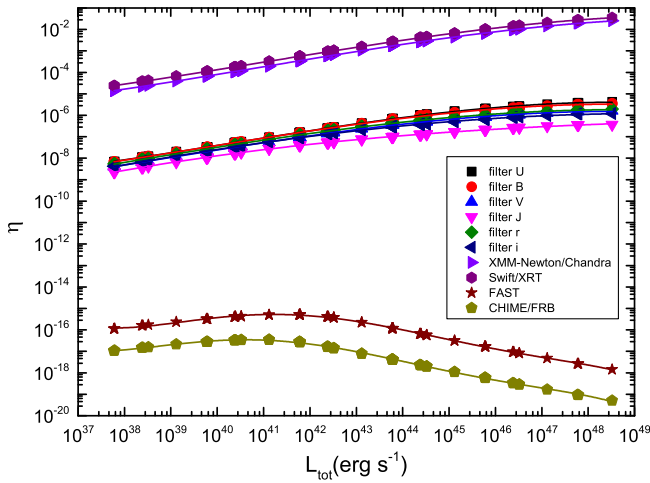
and increases with L_{tot} in x-ray, UV, and near-infrared. However, the conversion efficiency in the radio band initially increase slowly, and then decreases with L_{tot}.

B. Constraining the charge of a BH: Application for the GW200105 and GW200115 events

Based on the Eqs. (4) and (8), the $L_{\text{tot}} = L_e + L_m$ is dependent on the charge and mass of both the BH and NS. The charge of the NS (Q_{NS}) also depends on the parameters of the NS, e.g., period, the strength of magnetic field, and the radius, but we know little about those parameters. In order to test the magnitude of Q_{NS}, we fix the radius $R_{\text{NS}} = 12$ km, and adopt five groups of typical period ($P = 1$ ms, 5 ms, 10 ms, 50 ms, and 100 ms) and strength of magnetic field ($B_p = 10^{12}$ G, 10^{13} G, 10^{14} G, 10^{15} G, and 10^{16} G). Then we calculated the NS charge using various combinations of the above parameters.

Applying this analysis to the GW200105 and GW200115 events, we can estimate the parameters of the BH and NS (e.g., mass of the BH and NS, luminosity distance, mass ratio, and chirp mass) via the GW observations. On the other hand, by assuming that the observed optical transients or even upper limits in Sec. III are the EM counterparts of the GW200105 and GW200115 events, then, we can calculate the luminosity (L_{obs}) based on the luminosity distance[5] and observed magnitude in the optical/IR band. Here, we calculate the L_{obs} by adopting the maximum and minimum magnitudes in the optical/IR in Tables II and III as marked $L_{\text{obs,max}}$ and $L_{\text{obs,min}}$, respectively. The range of L_{obs} is $L_{\text{obs,min}} < L_{\text{obs}} < L_{\text{obs,max}}$, and adopt L_{obs} corresponding L_ν. Based on the Fig. 1, one can roughly estimate the conversion efficiency in the optical/IR bands. Combining with Eqs. (4)–(8), one can derive the luminosity of electric and magnetic dipole radiation at each orbital separation (a). Then, we take the sum of the luminosity at each orbital separation as the injected energy of Poynting-flux-dominated outflow. Finally, by adopting Eqs. (11)–(17), one can roughly estimate the charge on the BH for $L_\nu = L_{\text{obs,min}}$ and $L_\nu = L_{\text{obs,max}}$. The results are presented in Table IV. In this table, we define $\hat{q}_{\text{BH,1}}$ and $\hat{q}_{\text{BH,2}}$ in units of $Q_{\text{BH}}/M_{\text{BH}}$ (the charge for unit mass) are derived by the magnitude of the brightest and dimmest EM candidates for GW 200105 and GW200115, respectively.

For GW200105, we find that the estimated maximal charge-to-mass ratio of BH is between 9.73×10^{-8} and 1.12×10^{-6} esu with $B_p \lesssim 10^{16}$ G and $P > 1$ ms for the NS. Similarly, for GW200115, we also estimate the maximal charge-to-mass ratio of BH which ranges from 8.84×10^{-8} to 1.53×10^{-6} esu with $B_p \lesssim 10^{16}$ G and $P > 1$ ms for the NS.

FIG. 1. η as a function with L_{tot} for different energy bands.

TABLE IV. BH charge for GW200105 and GW200115 with different NS B_p and P.

			GW200105		
			P (ms)		
			$\hat{q}_{BH}(esu)^{a}$		
B_p (G)		1	5	10	50	100

B_p (G)		1	5	10	50	100
10^{12}	$\hat{q}_{BH,1}$	4.86×10^{-7}	4.86×10^{-7}	4.86×10^{-7}	4.86×10^{-7}	4.86×10^{-7}
	$\hat{q}_{BH,2}$	9.74×10^{-8}	9.73×10^{-8}	9.73×10^{-8}	9.73×10^{-8}	9.73×10^{-8}
10^{13}	$\hat{q}_{BH,1}$	4.87×10^{-7}	4.86×10^{-7}	4.86×10^{-7}	4.86×10^{-7}	4.86×10^{-7}
	$\hat{q}_{BH,2}$	9.79×10^{-8}	9.74×10^{-8}	9.74×10^{-8}	9.74×10^{-8}	9.73×10^{-8}
10^{14}	$\hat{q}_{BH,1}$	4.93×10^{-7}	4.87×10^{-7}	4.87×10^{-7}	4.86×10^{-7}	4.86×10^{-7}
	$\hat{q}_{BH,2}$	1.04×10^{-7}	9.86×10^{-8}	9.79×10^{-8}	9.74×10^{-8}	9.74×10^{-8}
10^{15}	$\hat{q}_{BH,1}$	5.50×10^{-7}	4.99×10^{-7}	4.93×10^{-7}	4.87×10^{-7}	4.87×10^{-7}
	$\hat{q}_{BH,2}$	1.61×10^{-7}	1.10×10^{-7}	1.04×10^{-7}	9.86×10^{-8}	9.79×10^{-8}
10^{16}	$\hat{q}_{BH,1}$	1.12×10^{-6}	6.13×10^{-7}	5.50×10^{-7}	4.99×10^{-7}	4.93×10^{-7}
	$\hat{q}_{BH,2}$	5.38×10^{-7}	2.24×10^{-7}	1.61×10^{-7}	1.10×10^{-7}	1.04×10^{-7}
				GW200115		
10^{12}	$\hat{q}_{BH,1}$	6.69×10^{-7}	6.69×10^{-7}	6.69×10^{-7}	6.69×10^{-7}	6.69×10^{-7}
	$\hat{q}_{BH,2}$	8.85×10^{-8}	8.84×10^{-8}	8.84×10^{-8}	8.84×10^{-8}	8.84×10^{-8}
10^{13}	$\hat{q}_{BH,1}$	6.70×10^{-7}	6.69×10^{-7}	6.69×10^{-7}	6.69×10^{-7}	6.69×10^{-7}
	$\hat{q}_{BH,2}$	8.93×10^{-8}	8.86×10^{-8}	8.85×10^{-8}	8.84×10^{-8}	8.84×10^{-8}
10^{14}	$\hat{q}_{BH,1}$	6.78×10^{-7}	6.71×10^{-7}	6.70×10^{-7}	6.69×10^{-7}	6.69×10^{-7}
	$\hat{q}_{BH,2}$	9.70×10^{-8}	9.01×10^{-8}	8.93×10^{-8}	8.86×10^{-8}	8.85×10^{-8}
10^{15}	$\hat{q}_{BH,1}$	7.55×10^{-7}	6.86×10^{-7}	6.78×10^{-7}	6.71×10^{-7}	6.70×10^{-7}
	$\hat{q}_{BH,2}$	1.75×10^{-7}	1.06×10^{-7}	9.70×10^{-8}	9.01×10^{-8}	8.93×10^{-8}
10^{16}	$\hat{q}_{BH,1}$	1.53×10^{-6}	8.41×10^{-7}	7.55×10^{-7}	6.86×10^{-7}	6.78×10^{-7}
	$\hat{q}_{BH,2}$	9.50×10^{-7}	2.61×10^{-7}	1.75×10^{-7}	1.06×10^{-7}	9.70×10^{-8}

[a]Derived the BH charge for given B_p and P of NS. $\hat{q}_{BH,1}$ and $\hat{q}_{BH,2}$ *in unit of* Q_{BH}/M_{BH} (the charge for unit mass) are derived by the magnitude of the brightest and dimmest EM candidates for GW 200105 and GW200115, respectively.

V. CONCLUSION AND DISCUSSION

The physical properties of any BH can be described with its mass, angular momentum, and charge. The mass and angular momentum of the BH can be roughly measured based on currently observed data, but to infer the charge of a BH remains an open question. One proposal is that a charged BH and NS merger could be a potential approach to constrain the BH charge [40]. Recently, two GW events (GW200105 and GW200115) originating from the merger of a BH-NS system are confirmed to be detected by aLIGO and Virgo, and several optical source candidates are reported to possible associate with the two GW events, but not confirmed yet. In this paper, by assuming that the possible optical sources are associated with GW200105 and GW200115, we try to estimate the BH charge via the observed upper limits of the EM radiation in the charged BH and NS system.

A charged BH merging with a NS can produce electric and magnetic dipole radiation. Then, the energy from the electric and magnetic dipole radiation injects into the outflow which is Poynting-flux dominated, and the magnetic energy can convert into the kinetic energy of electrons by magnetic reconnection and turbulence to accelerate electrons. It can produce the observed EM radiation by assuming synchrotron radiation in the outflow. Within this scenario, we calculate the conversion efficiency of the electric dipole and magnetic dipole radiation within different energy bands, and constrain the BH charge for given NS physical parameters (e.g., period and surface magnetic field). The following interesting results are obtained.

(i) We find that the conversion efficiency in the x-ray band is much higher than that of the ultraviolet (UV), near-infrared, and radio bands, and it increases with L_{tot} in the x-ray, UV, and near-infrared. However, the conversion efficiency in the radio band initially increases slowly, and then decreases with L_{tot}.

(ii) For GW200105, we find that the estimated maximal charge-to-mass ratio (the charge for unit mass) of the BH is between about 9.73×10^{-8} and 1.12×10^{-6}

esu with $B_p \lesssim 10^{16}$ G and $P > 1$ ms for the NS. Similarly, for GW200115, we also estimate the maximal charge-to-mass ratio of the BH which ranges from 8.84×10^{-8} to 1.53×10^{-6} esu with $B_p \lesssim 10^{16}$ G and $P > 1$ ms for the NS.

In fact, the radiation is only found in the leading order post-Newtonian expansion, which for the electric dipole is even lower order (-1PN) than the GW quadrupole. In our calculations, we do not consider the contribution of EM force for modification of the orbit, because the EM force is much smaller than gravitational force in our analysis. However, the contribution of EM force is not negligible if EM and gravitational forces are comparable between each other [51,52].

It has always been expected to be able to simultaneously observe GW and EM signals from BH-NS merger systems, and to search for the EM counterparts of the GW event from such mergers remains an interesting and hot topic in astrophysics. Reference [101] proposed that the NS charge can be transformed to the BH during inspiral phase of the BH-NS system. Within this scenario, the calculated BH charge in this work is underestimated, and it means that we do not consider the charge contributed by the magneto-sphere of the NS within the BH-NS system. Within the scenario of charged BH-NS systems, the people have theoretically studied the EM and GW radiations in its different evolutional phase through numerical Einstein-Maxwell equations. Reference [102] simulated charged-black hole head-on collisions with the equal charge-to-mass ratio. They found that the ratio of energy carried between GW and EM radiations would decrease with the increasing of charge-to-mass ratio. Reference [103] considered the quasicircular inspiral and merger of charged BH-BH systems and derived the similar outcomes. These works stated that the EM force is negligible when the charge-to-mass ratio is small enough, and it is consistent with our assumptions.

On the other hand, some researchers also try to constrain the charge of supermassive black holes that reside in the central of galaxies, e.g., Sgr A* and M87* [104,105]. Reference [105] considered Sgr A* as a Kerr-Newman black to constrain the supermassive black hole charge based on the Event Horizon Telescope observation of the shadow. Similarly, Refs. [106,107] constrain the quantity of supermassive black hole charge which is less than 3.1×10^8 C by using Chandra x-ray data.

Moreover, by adopting the estimated parameters via possible optical counterparts for the GW200105 and GW200115 events, we calculate the possibility of detection in the radio and x-ray bands by comparing with the sensitivities of Five-hundred-meter Aperture Spherical radio Telescope (FAST) and Swift/XRT, respectively. We find that the FAST can not be triggered with fixed $P = 1$ ms and $B_p = 10^{16}$ G for the NS, but it is expected to detected by Swift/XRT. The reason may be the lower conversion efficiency of the dipole radiation in the radio band. The results are shown in Fig. 2.

Owing to absence of a simultaneous observation of GW emission and any EM counterparts from a BH-NS merger system, to understand their properties remains an open question. However, it is necessary to study first in theory before discovering any GW emission associated with EM in the observations in such BH-NS systems. Due to the higher conversion efficiency of the dipole radiation in the x-ray band, we encourage the space based x-ray telescopes to follow-up observations of GW events from BH-NS merger systems. Troja *et al.* [108] stated that there would be a precursor emission before merger of binary neutron star. If the dipole radiations really exist during the inspiral and merger of charged binary compact star, the precursor emission would be another way to test our research and probe the properties of charged compact star systems. Moreover, the next generation GW detectors, e.g., Cosmic Explorer [109] and the Einstein Telescope [110,111], are also expected to be more sensitive and the higher sky-localization ability will provide guidance for the follow-up EM observations.

One needs to note that the fundamental of this work is the existing BH-NS events. The several candidates (GW 190426, GW 190814, GW 190917, GW 191219, and GW 200210) as the BH-NS events remain in debate due to the high mass of secondary [68]. Also, GW 200105 is also debating that whether it is a BH-NS event or not due to the high likelihood of detector noise [68]. The LIGO pipeline considers anything below 3 solar mass as a neutron star, while the maximum mass of neutron stars is nearly certainly lower than that. So that, we expect that more confirmed BH-NS events can be detected by LVC in the future.
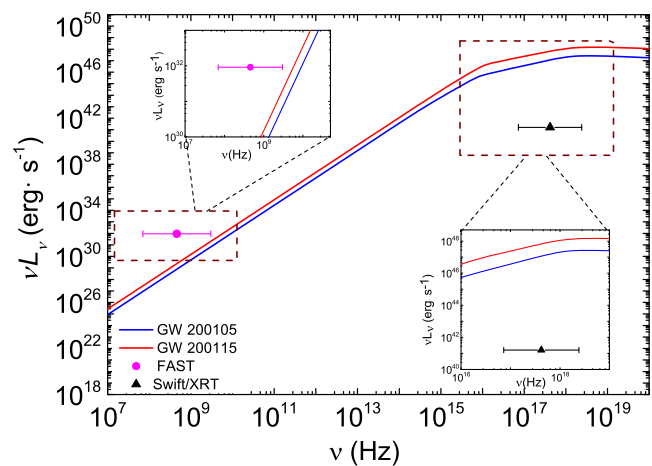

FIG. 2. Comparing the FAST and Swift/XRT sensitivity with the luminosity calculated by the method mentioned in Sec. II. We fix the NS parameters as $P = 1$ ms and $B_p = 10^{16}$ G for both GW200105 and GW200115 events.

[1] E. Berger, Annu. Rev. Astron. Astrophys. **52**, 43 (2014).

[2] J. Aasi, B. P. Abbott *et al.* (LIGO Scientific Collaboration), Classical Quantum Gravity **32**, 074001 (2015).

[3] F. Acernese, M. Agathos, K. Agatsuma *et al.*, Classical Quantum Gravity **32**, 024001 (2015).

[4] Y. Aso, Y. Michimura, K. Somiya, M. Ando, O. Miyakawa, T. Sekiguchi, D. Tatsumi, and H. Yamamoto, Phys. Rev. D **88**, 043007 (2013).

[5] B. P. Abbott, R. Abbott, T. D. Abbott *et al.*, Phys. Rev. Lett. **116**, 131103 (2016).

[6] V. Connaughton, E. Burns, A. Goldstein *et al.*, Astrophys. J. Lett. **826**, L6 (2016).

[7] M. Lyutikov, arXiv:1602.07352.

[8] J. Greiner, J. M. Burgess, V. Savchenko, and H.-F. Yu, Astrophys. J. Lett. **827**, L38 (2016).

[9] B. P. Abbott, R. Abbott, T. D. Abbott *et al.*, Astrophys. J. Lett. **848**, L13 (2017).

[10] B. P. Abbott, R. Abbott, T. D. Abbott *et al.*, Phys. Rev. Lett. **119**, 161101 (2017).

[11] A. Goldstein, P. Veres, E. Burns *et al.*, Astrophys. J. Lett. **848**, L14 (2017).

[12] V. Savchenko, C. Ferrigno, E. Kuulkers *et al.*, Astrophys. J. Lett. **848**, L15 (2017).

[13] R. Chornock, E. Berger, D. Kasen *et al.*, Astrophys. J. Lett. **848**, L19 (2017).

[14] D. A. Coulter, R. J. Foley, C. D. Kilpatrick *et al.*, Science **358**, 1556 (2017).

[15] S. Covino, K. Wiersema, Y. Z. Fan *et al.*, Nat. Astron. **1**, 791 (2017).

[16] B.-B. Zhang, B. Zhang, H. Sun *et al.*, Nat. Commun. **9**, 447 (2018).

[17] Y.-J. Li, M.-Z. Han, S.-P. Tang *et al.*, arXiv:2012.04978.

[18] R. Abbott, T. D. Abbott, S. Abraham *et al.*, Astrophys. J. Lett. **896**, L44 (2020).

[19] R. Abbott *et al.* (The LIGO Scientific Collaboration and the Virgo Collaboration), arXiv:2108.01045.

[20] B. P. Gompertz, M. Nicholl, P. Schmidt, G. Pratten, and A. Vecchio, Mon. Not. R. Astron. Soc. **511**, 1454 (2022).

[21] M. U. Kruckow and Z. Han, arXiv:2112.07847.

[22] R. Abbott, T. D. Abbott, S. Abraham *et al.*, Astrophys. J. Lett. **915**, L5 (2021).

[23] S. Anand, M. W. Coughlin, M. M. Kasliwal *et al.*, Nat. Astron. **5**, 46 (2021).

[24] K. D. Alexander, G. Schroeder, K. Paterson *et al.*, Astrophys. J. **923**, 66 (2021).

[25] M. W. Coughlin, T. Dietrich, S. Antier *et al.*, Mon. Not. R. Astron. Soc. **497**, 1181 (2020).

[26] B. P. Gompertz, R. Cutter, D. Steeghs *et al.*, Mon. Not. R. Astron. Soc. **497**, 726 (2020).

[27] M. M. Kasliwal, S. Anand, T. Ahumada *et al.*, Astrophys. J. **905**, 145 (2020).

[28] K. L. Page, P. A. Evans, A. Tohuvavohu *et al.*, Mon. Not. R. Astron. Soc. **499**, 3459 (2020).

[29] A. L. Thakur, S. Dichiara, E. Troja *et al.*, Mon. Not. R. Astron. Soc. **499**, 3868 (2020).

[30] D. Dobie, A. Stewart, K. Hotokezaka *et al.*, Mon. Not. R. Astron. Soc. **510**, 3794 (2022).

[31] F. Foucart, Phys. Rev. D **86**, 124007 (2012).

[32] F. Foucart, M. B. Deaton, M. D. Duez, L. E. Kidder, I. MacDonald, C. D. Ott, H. P. Pfeiffer, M. A. Scheel, B. Szilagyi, and S. A. Teukolsky, Phys. Rev. D **87**, 084006 (2013).

[33] G. Fragione, Astrophys. J. Lett. **923**, L2 (2021).

[34] D. J. D'Orazio, Z. Haiman, J. Levin, J. Samsing, and A. Vigna-Gómez, Astrophys. J. **927**, 56 (2022).

[35] P. D. Lasky, B. Haskell, V. Ravi, E. J. Howell, and D. M. Coward, Phys. Rev. D **89**, 047302 (2014).

[36] H.-J. Lü, B. Zhang, W.-H. Lei, Y. Li, and P. D Lasky, Astrophys. J. **805**, 89 (2015).

[37] H.-J. Lü, H.-M. Zhang, S.-Q. Zhong, S.-J. Hou, H. Sun, J. Rice, and E.-W. Liang, Astrophys. J. **835**, 181 (2017).

[38] B. P. Abbott, R. Abbott, T. D. Abbott *et al.*, Phys. Rev. Lett. **121**, 161101 (2018).

[39] R. Abbott, T. D. Abbott, S. Abraham *et al.*, Astrophys. J. Lett. **913**, L7 (2021).

[40] B. Zhang, Astrophys. J. Lett. **873**, L9 (2019).

[41] S. L. Shapiro and S. A. Teukolsky, *A Wiley-Interscience Publication* (Wiley, New York, 1983).

[42] K. Inayoshi, E. Visbal, and Z. Haiman, Annu. Rev. Astron. Astrophys. **58**, 27 (2020).

[43] Y. Feng, X. Zhao, L. Gou, J. Wu, J. F. Steiner, Y. Li, Z. Liao, N. Jia, and Y. Wang, Astrophys. J. **925**, 142 (2022).

[44] N. Aghanim, Y. Akrami *et al.* (Planck Collaboration), Astron. Astrophys. **641**, A6 (2020).

[45] K. Kyutoku, M. Shibata, and K. Taniguchi, Living Rev. Relativity **24**, 5 (2021).

[46] M. Shibata and K. Hotokezaka, Annu. Rev. Nucl. Part. Sci. **69**, 41 (2019).

[47] M. J. Benacquista and J. M. B. Downing, Living Rev. Relativity **16**, 4 (2013).

[48] B. Zhang, Astrophys. J. Lett. **827**, L31 (2016).

[49] C.-M. Deng, Y. Cai, X.-F. Wu, and E.-W. Liang, Phys. Rev. D **98**, 123016 (2018).

[50] V. Cardoso, C. F. B. Macedo, P. Pani, and V. Ferrari, J. Cosmol. Astropart. Phys. 05 (**2016**) 054.

[51] L. Liu, Z.-K. Guo, R.-G. Cai *et al.*, Phys. Rev. D **102,** 043508 (2020).

[52] Ø. Christiansen, J. B. Jiménez, and D. F. Mota, Classical Quantum Gravity **38,** 075017 (2021).

[53] M. Zajaček, A. Tursunov, A. Eckart, S. Britzen, E. Hackmann, V. Karas, Z. Stuchlík, B. Czerny, and J. A. Zensus, J. Phys. Conf. Ser. **1258,** 012031 (2019).

[54] L. Bildsten and C. Cutler, Astrophys. J. **400,** 175 (1992).

[55] C. S. Kochanek, Astrophys. J. **398,** 234 (1992).

[56] P. Goldreich and W. H. Julian, Astrophys. J. **157,** 869 (1969).

[57] M. A. Ruderman and P. G. Sutherland, Astrophys. J. **196,** 51 (1975).

[58] V. Cardoso, W.-D. Guo, C. F. B. Macedo, and P. Pani, Mon. Not. R. Astron. Soc. **503,** 563 (2021).

[59] P. Beniamini and D. Giannios, Mon. Not. R. Astron. Soc. **468,** 3202 (2017).

[60] D. Giannios and H. C. Spruit, Astron. Astrophys. **430,** 1 (2005).

[61] L. Sironi and A. Spitkovsky, Astrophys. J. Lett. **783,** L21 (2014).

[62] F. Guo, Y.-H. Liu, W. Daughton, and H. Li, Astrophys. J. **806,** 167 (2015).

[63] G. R. Werner, D. A. Uzdensky, B. Cerutti *et al.*, Astrophys. J. Lett. **816,** L8 (2016).

[64] B. Zhang, *The Physics of Gamma-Ray Bursts by Bing Zhang* (Cambridge Univeristy Press, Cambridge, England, 2018), ISBN: 978-1-139-22653-0, 10.1017/9781139226530.

[65] D. Xiao and Z.-G. Dai, Astrophys. J. **846,** 130 (2017).

[66] R. Sari, T. Piran, and R. Narayan, Astrophys. J. Lett. **497,** L17 (1998).

[67] J. Granot and R. Sari, Astrophys. J. **568,** 820 (2002).

[68] The LIGO Scientific Collaboration, the Virgo Collaboration, the KAGRA Collaboration *et al.*, arXiv:2111.03606.

[69] M. Doyle, A. Martin-Carrillo, V. Savchenko *et al.*, GCN, Circular Service, No. 26644, 1, 2020.

[70] P. Veres (Fermi-GBM Team and GBM-LIGO/Virgo Group), GCN, Circular Service, No. 26645, 1, 2020.

[71] F. Lucarelli (Agile Team), GCN, Circular Service, No. 26647, 1, 2020.

[72] S. D. Barthelmy (Swift Team), GCN, Circular Service, No. 26649, 1, 2020.

[73] HAWC Collaboration, GCN, Circular Service, No. 26758, 1, 2020.

[74] HAWC Collaboration, GCN, Circular Service, No. 26650, 1, 2020.

[75] V. Shenoy (AstroSat CZTI Collaboration), GCN, Circular Service, No. 26652, 1, 2020.

[76] K. Yamaoka, A. Yoshida, T. Sakamoto *et al.*, GCN, Circular Service, No. 26664, 1, 2020.

[77] A. Ridnaia, S. Golenetskii, R. Aptekar *et al.*, GCN, Circular Service, No. 26849, 1, 2020.

[78] A. Ridnaia, S. Golenetskii, R. Aptekar *et al.*, GCN, Circular Service, No. 26837, 1, 2020.

[79] A. Ursi, F. Verrecchia, C. Pittori *et al.*, GCN, Circular Service, No. 26765, 1, 2020.

[80] A. Ursi, C. Pittori, F. Verrecchia *et al.*, GCN, Circular Service, No. 26769, 1, 2020.

[81] C. Ferrigno, V. Savchenko, S. Mereghetti *et al.*, GCN, Circular Service, No. 26766, 1, 2020.

[82] A. Goldstein (Fermi-GBM Team and GBM-LIGO/Virgo Group), GCN, Circular Service, No. 26774, 1, 2020.

[83] M. Crnogorcevic (Fermi-LAT Collaboration), GCN, Circular Service, No. 26775, 1, 2020.

[84] T. Sakamoto (Swift Team), GCN, Circular Service, No. 26779, 1, 2020.

[85] Y. Shimizu, A. Yoshida, T. Sakamoto *et al.*, GCN, Circular Service, No. 26797, 1, 2020.

[86] S. Sugita, M. Serino (MAXI Team), GCN, Circular Service, No. 26651, 1, 2020.

[87] N. Kawai (MAXI Team), GRB Coordinates Network, Circular Service, No. 26760, 2020.

[88] P. A. Evans (Swift Team), GCN, Circular Service, No. 26855, 1, 2020.

[89] P. A. Evans (Swift Team), GCN, Circular Service, No. 26798, 1, 2020.

[90] V. Lipunov, E. Gorbovskoy, V. Kornilov *et al.*, GCN, Circular Service, No. 26646, 1, 2020.

[91] R. Stein (ZTF Collaboration and Growth Collaboration), GCN, Circular Service, No. 26673, 1, 2020.

[92] T. Ahumada, GCN, Circular Service, No. 26810, 1, 2020.

[93] A. F. Valeev and J. Font, GCN, Circular Service, No. 26702, 1, 2020.

[94] A. J. Castro-Tirado and J. Font, GCN, Circular Service, No. 26703, 1, 2020.

[95] I. Andreoni, GCN, Circular Service, No. 26863, 1, 2020.

[96] S. Anand (Zwicky Transient Facility (ZTF) Collaboration and Global Relay Of Observatories Watching Transients Happen (Growth) Collaboration), GCN, Circular Service, No. 26767, 1, 2020.

[97] S. Srivastav and S. J. Smartt, GCN, Circular Service, No. 26839, 1, 2020.

[98] Y.-D. Hu, Caballero M. D. Garcia, J. Font *et al.*, GCN, Circular Service, No. 26701, 1, 2020.

[99] J. L. Tonry, C. W. Stubbs, K. R. Lykke *et al.*, Astrophys. J. **750,** 99 (2012).

[100] S. R. Oates (Swift Team), GCN, Circular Service, No. 26808, 1, 2020.

[101] K. Chen and Z. G. Dai, Astrophys. J. **909,** 4 (2021).

[102] M. Zilhão, V. Cardoso, C. Herdeiro, L. Lehner, and U. Sperhake, Phys. Rev. D **85,** 124062 (2012).

[103] G. Bozzola and V. Paschalidis, Phys. Rev. D **104,** 044004 (2021).

[104] P. Kocherlakota, L. Rezzolla, H. Falcke *et al.*, Phys. Rev. D **103,** 104047 (2021).

[105] S. G. Ghosh and M. Afrin, Astrophys. J. **944,** 174 (2023).

[106] M. Karouzos, Nat. Astron. **2,** 764 (2018).

[107] M. Zajaček, A. Tursunov, A. Eckart, and S. Britzen, Mon. Not. R. Astron. Soc. **480,** 4408 (2018).

[108] E. Troja, S. Rosswog, and N. Gehrels, Astrophys. J. **723,** 1711 (2010).

[109] D. Reitze, R. X. Adhikari, S. Ballmer *et al.*, Bull. Am. Astron. Soc. **51,** 35 (2019).

[110] M. Punturo, M. Abernathy, F. Acernese *et al.*, Classical Quantum Gravity **27,** 084007 (2010).

[111] M. Punturo, M. Abernathy, F. Acernese *et al.*, Classical Quantum Gravity **27,** 194002 (2010).